



This open access document is posted as a preprint in the Beilstein Archives at <https://doi.org/10.3762/bxiv.2023.53.v1> and is considered to be an early communication for feedback before peer review. Before citing this document, please check if a final, peer-reviewed version has been published.

This document is not formatted, has not undergone copyediting or typesetting, and may contain errors, unsubstantiated scientific claims or preliminary data.

Preprint Title Facile Approach to the N,O,S-Heteropentacycles via Condensation of Sterically Crowded 3H-Phenoxazin-3-one with *ortho*-amino-, hydroxy- and mercaptoanilines

Authors Eugeny P. Ivakhnenko, Vasily I. Malay, Pavel A. Knyazev, Nikita I. Merezhko, Nadezhda I. Makarova, Oleg P. Demidov, Gennady S. Borodkin, Andrey G. Starikov and Vladimir I. Minkin

Publication Date 27 Nov 2023

Article Type Full Research Paper

Supporting Information File 1 SI BJOC.docx; 8.5 MB

ORCID® iDs Eugeny P. Ivakhnenko - <https://orcid.org/0000-0003-0338-6466>; Vasily I. Malay - <https://orcid.org/0000-0002-5302-743X>; Pavel A. Knyazev - <https://orcid.org/0000-0001-6627-8329>; Nikita I. Merezhko - <https://orcid.org/0009-0000-2672-4072>; Nadezhda I. Makarova - <https://orcid.org/0000-0002-7196-9842>; Oleg P. Demidov - <https://orcid.org/0000-0002-3586-0487>; Gennady S. Borodkin - <https://orcid.org/0000-0002-5886-7825>; Andrey G. Starikov - <https://orcid.org/0000-0002-5613-6308>; Vladimir I. Minkin - <https://orcid.org/0000-0001-6096-503X>



License and Terms: This document is copyright 2023 the Author(s); licensee Beilstein-Institut.

This is an open access work under the terms of the Creative Commons Attribution License (<https://creativecommons.org/licenses/by/4.0>). Please note that the reuse, redistribution and reproduction in particular requires that the author(s) and source are credited and that individual graphics may be subject to special legal provisions.

The license is subject to the Beilstein Archives terms and conditions: <https://www.beilstein-archives.org/xiv/terms>.

The definitive version of this work can be found at <https://doi.org/10.3762/bxiv.2023.53.v1>

Facile Approach to the N,O,S-Heteropentacycles via Condensation of Sterically Crowded 3H-Phenoxazin- 3-one with *ortho*-amino-, hydroxy- and mercaptoanilines

Eugeny Ivakhnenko*¹, Vasily Malay¹, Pavel Knyazev¹, Nikita Merezhko¹, Nadezhda Makarova¹, Oleg Demidov², Gennady Borodkin¹, Andrey Starikov¹ and Vladimir Minkin¹

Address: ¹Institute of Physical and Organic Chemistry, Southern Federal University, 194/2 Stachki St., 344090, Rostov-on-Don, Russian Federation and ²North Caucasus Federal University, 1 Pushkin St., 355017, Stavropol, Russian Federation.

Email: Eugeny Ivakhnenko – ivakhnenko@sfedu.ru

* Corresponding author

Abstract

A convenient method for the synthesis of a series of 2-arylamino-3H-phenoxazin-3-ones based on the nucleophilic substitution reaction between sterically crowded 3H-phenoxazin-3-one and arylamines performed by short-term heating of the melted reactants at 230-250 °C is described and the compounds are characterized by means of single-crystal X-ray crystallography, NMR, UV/vis, IR spectroscopy and cyclic voltammetry. Involvement into the reaction of arylamines with *o*-amino-, *o*-hydroxy and

o-mercapto-substituents widens its scope and provides for an access to derivatives of N,O- and N,S-heteropentacyclic quinoxalinophenoxazine, triphenodioxazine and oxazinophenothiazine systems.

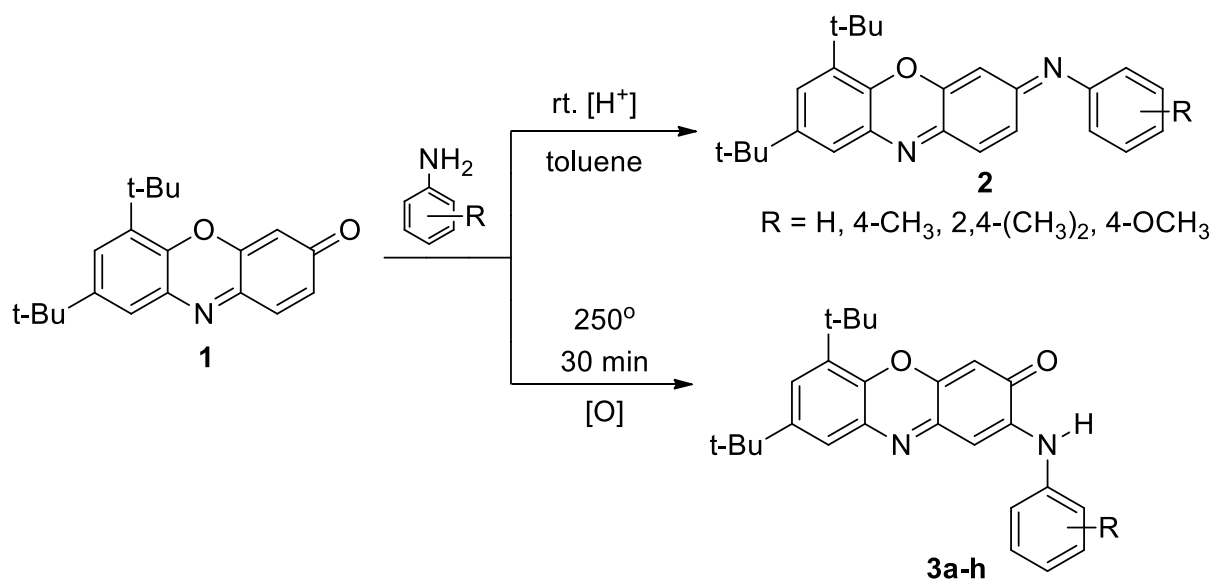
Keywords

3H-phenoxazin-3-one; pentacyclic heterocycles; synthesis; fluorescence; molecular structure

Introduction

3H-phenoxazin-3-one and its derivatives widely distributed in the natural world in microorganisms and fungi represent the key structural units of a number of important drugs with antibacterial, antifungal, anticancer, anti-inflammatory and antiviral activities [1,2]. Due to the presence in their molecules of several active reaction centers (Fig. 1) 3H-phenoxazin-3-ones easily accessed through the oxidation couplings of *o*-aminophenols [3, 4] or N-aryl-*o*-benzoquinone imines [5, 6] can serve as efficient precursors to pentacyclic N, O-heterocyclic compounds possessing promising properties for application in fluorescent probe, organic light-emitting diode and organic solar cells devices [2, 7-9]. The principal way to the formation of these compounds is the nucleophilic addition of aromatic amines to 3H-phenoxazin-3-ones and the subsequent cyclization of the initially formed adducts [10-12]. Reactivity of 3H-phenoxazin-3-ones is primarily determined by the properties of its *p*-quinone imine moiety. Therefore, these compounds can react with nucleophiles, in particular with amines, via one of the three pathways: Schiff base formation (attack at C(3) center), Michael type addition (at C(4)) or nucleophilic substitution (S_NH) at C(2) center [13-15]. The chose of one of the paths is strongly depends on the reaction conditions and

electrophilicity of the reaction centers C(1) – C(3) of a derivative of 6,8-di-*tert*-butyl-3H-phenoxazin-3-one **1**. Condensation of **1** with aromatic amines performed in toluene solution in the presence of catalytic amounts of *p*-toluenesulfonic acid affords (*E*)-*N*-(6,8-di-*tert*-butyl-3H-phenoxazin-3-ylidene)anilines **2** but proceeds smoothly only with highly basic amines [6] (Scheme 1).



Scheme 1: Synthesis of (6,8-di-*tert*-butyl)-3H-phenoxazin-3-ylidene)anilines [6] **2** and (6,8-di-*tert*-butyl)-2-arylamino-3H-phenoxazin-3-ones **3**.

As shown in Fig. 1 demonstrating distribution of the electronic density in a molecule of a 6,8-di-*tert*-butyl-3H-phenoxazin-3-one **1** (the basic compound for the following transformations studied in this work) the largest positive charge in this triad is concentrated at the C(2) atom. It comes, therefore, with no surprise that interaction of arylamines with 5-hydroxy and 5-acetoxy derivatives of 3H-phenoxazin-3-one is directed at its C(2) reaction center to yield 2-aminophenoxazinones as the final products at aerobic conditions [10, 16]. The reactions proceed readily on refluxing acidified (pK_a=1-5) ethanol solutions of the amine hydrochlorides to give 2-monosubstituted derivatives 2-(arylamino)-3H-phenoxazin-3-ones **3** in moderate yields. In the present work, we have suggested an improved procedure for the

synthesis of compounds **3** and extended it to arylamines with *o*-amino-, hydroxy- and mercapto-substituents to provide for the access to heteropolycyclic N, O, S-containing structures.

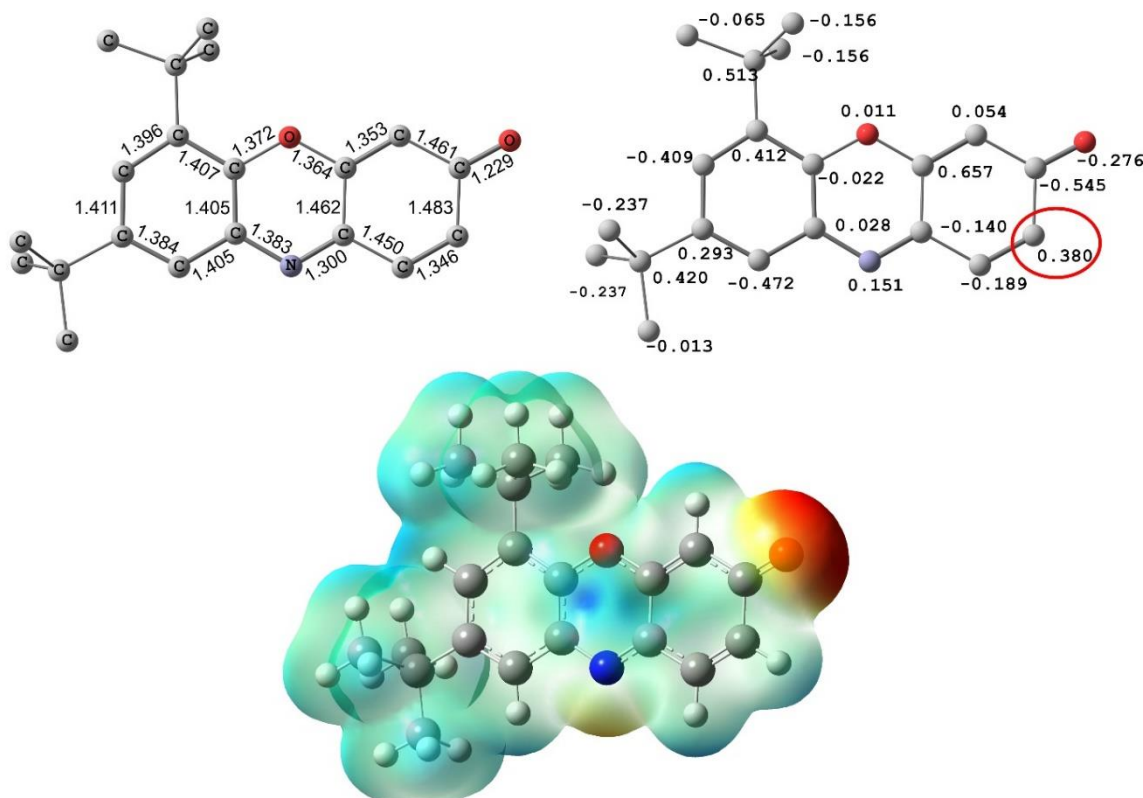
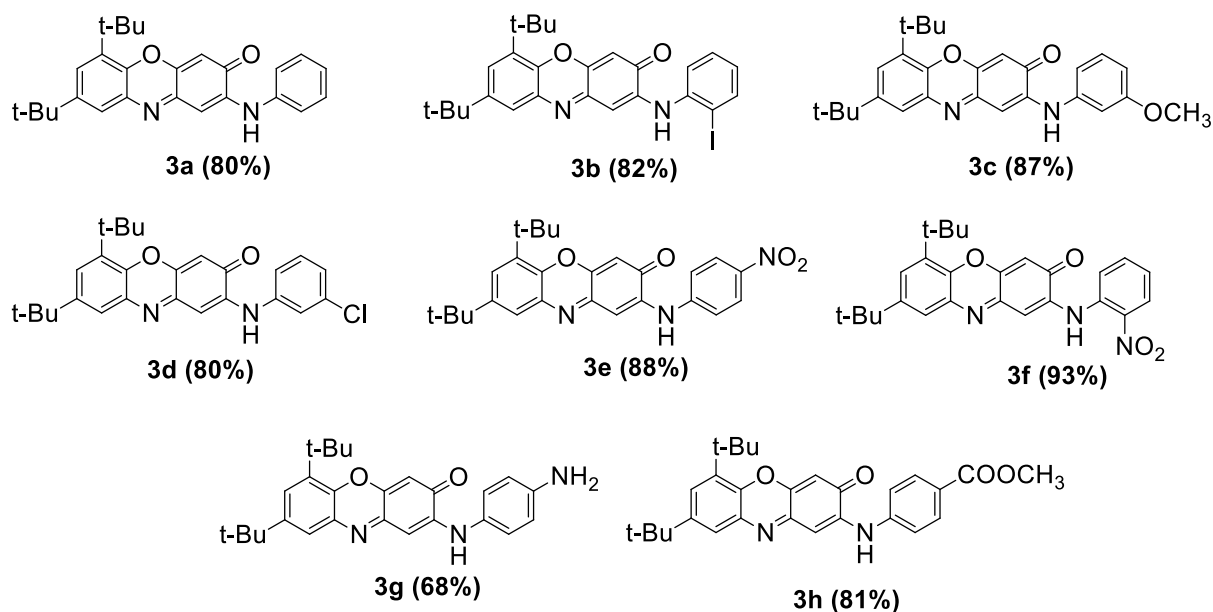


Figure 1: The DFT B3LYP/6-311++G(d,p) calculated molecular geometry and distribution of electronic density in a molecule of 6,8-di-*tert*-butyl-3H-phenoxazin-3-one
1: Mulliken charges and molecular electrostatic potential (isovalue=0.004).

Results and Discussion

We have found that a convenient way to a 2-arylamine-phenoxazin-3-ones **3** consists in a short-term heating (about 30 min) of the melted mixture of **1** and an arylamine at 250-270 °C followed by purification of the products on a chromatographic column. As seen from the data collected in Scheme 2, the nucleophilic substitution reaction occurs in good yields with no restrictions on basicity of the amines.



Scheme 2: 2-Arylamino-phenoxazin-3-ones **3** prepared by the one-pot reaction between 6,8-di-*tert*-butyl-3H-phenoxazin-3-one **1** and aromatic amines (the yields are given in brackets).

Molecular structures of compounds **3c,d,f** were X-ray determined and are shown in Fig. 2 (**3f**) and Figs. S1, S2 (**3c, 3d**). The geometry of the phenoxazine-one fragments of the compounds **3c,d,f** practically coincides with that found for 6,8-di-*tert*-butyl-3H-phenoxazin-3-one **1** [6]. A strong hydrogen bridge N(15)-H...O(31) is formed between the nitro and imino groups of the N-aryl ring.

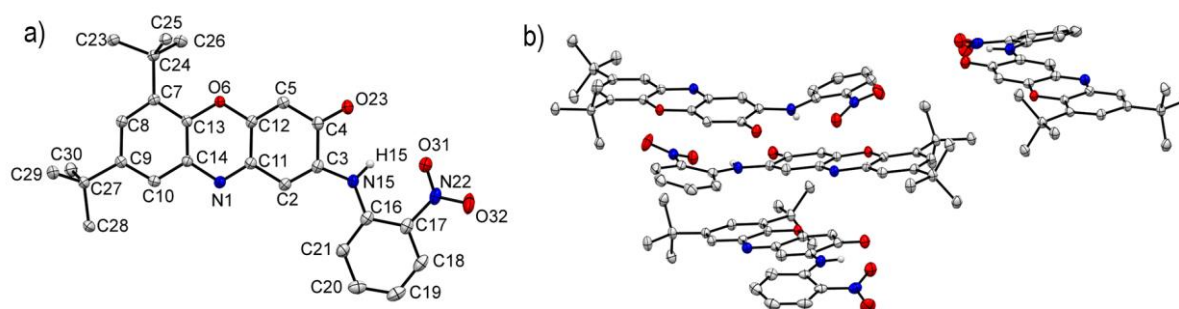


Figure 2: Molecular structure of 6,8-di-*tert*-butyl-2-(*o*-nitrophenylamino)-3H-phenoxazin-3-one **3f**. a) Selected bond distances: (Å) and angles: N1–C11 1.3061(19), N1–C14 1.3836(18), O23–C4 1.2314(19), N15–C3 1.3765(19), N15–C16 1.383(2), C11–N1–C14 117.55(12), C3–N15–C16 131.12(14). b) Package of molecules **3f** in crystal.

The main crystallographic parameters and bond distances are given in SI (Tables S1 and S4). Thermal ellipsoids are drawn at the 50% probability level.

The compounds **3a-h** intensely absorb light in the spectral range of 400-550 nm with maxima at 439-459 nm, $\epsilon = 20600\text{-}37100 \text{ M}^{-1}\cdot\text{cm}^{-1}$ (Fig. 3, Table 1). Introduction of an amino-group into *p*-position of the N-phenyl fragment gives rise to appearance of an additional long wavelength absorption band with $\lambda_{\text{max}} = 520 \text{ nm}$ and $\epsilon = 9200 \text{ M}^{-1} \text{ cm}^{-1}$.

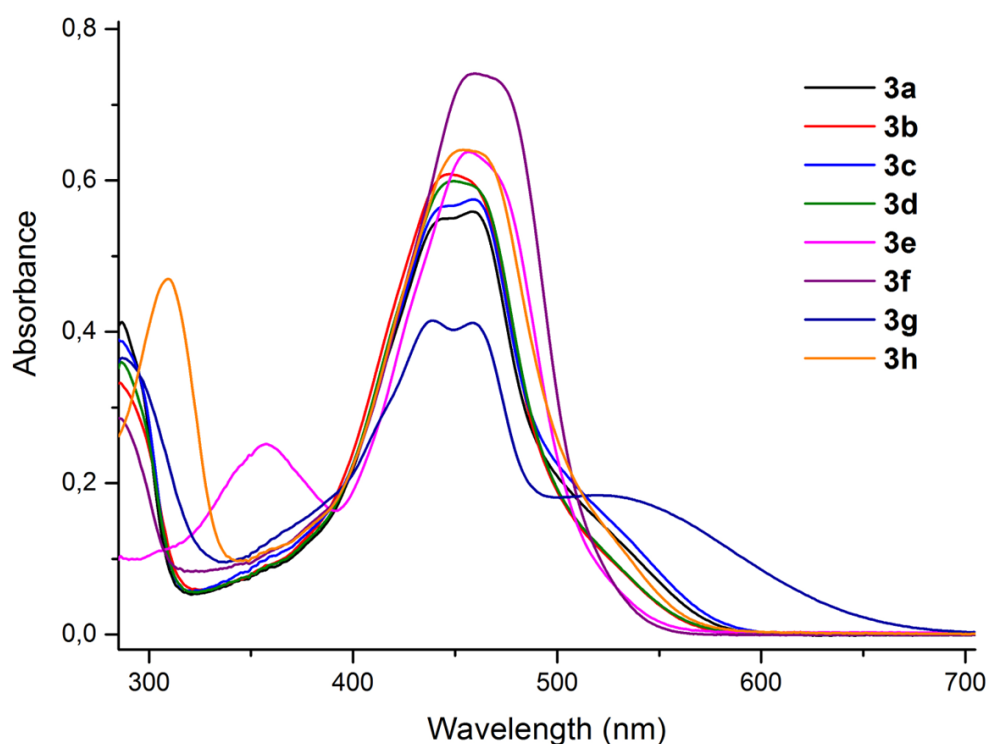


Figure 3: UV/vis spectra of 6,8-di-*tert*-butyl-2-arylamino-3H-phenoxazin-3-ones **3a-h** (toluene, $C = 2 \cdot 10^{-5} \text{ M}$, $l = 1 \text{ cm}$, $T = 293 \text{ K}$).

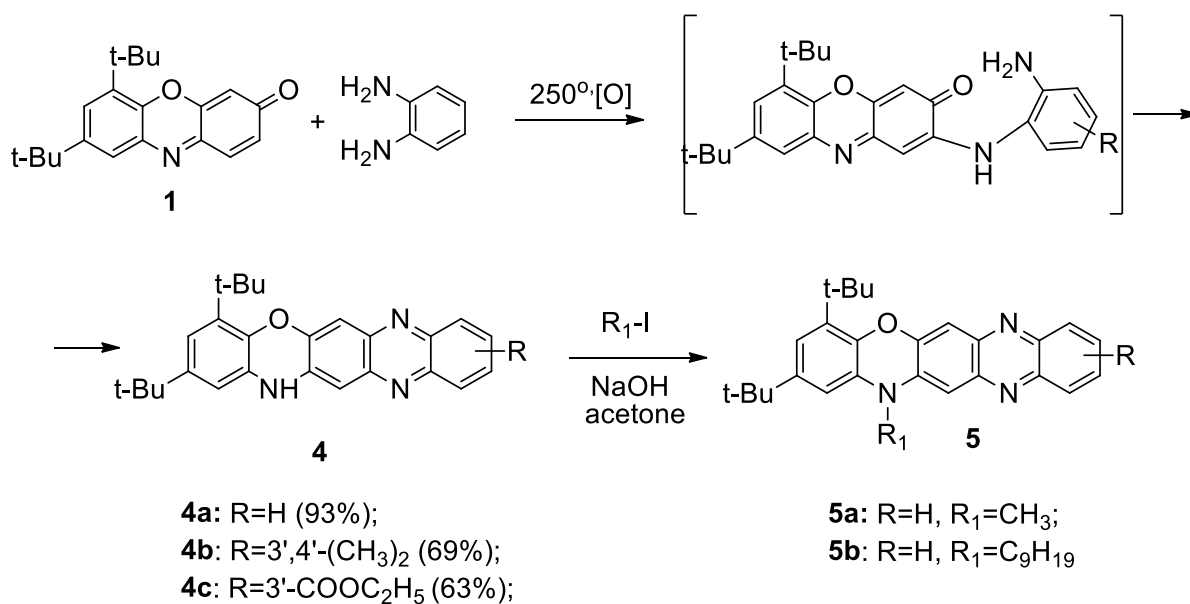
Table 1: UV/vis absorption data of (λ_{max} , ϵ) of 6,8-di-*tert*-butyl-2-arylamino-3H-phenoxazin-3-ones **3a-h** in toluene.

Compound	λ_{max} , nm ($\epsilon, 10^4 \text{ M}^{-1} \cdot \text{cm}^{-1}$)
3a	445 (2.75) ^{sh} , 458 (2.80)
3b	447 (3.04)
3c	444 (2.83) ^{sh} , 459 (2.88)

3d	449 (2.99)
3e	357 (1.26), 457 (3.19)
3f	459 (3.71)
3g	439 (2.07), 459 (2.06), 520 (0.92)
3h	309 (2.35), 454 (3.20)

^{sh}Shoulder

Involvement of *o*-phenylenediamine into reaction with 3*H*-phenoxazin-3-ones makes possible simultaneous activation of two principal reaction channels associated with S_NH and Schiff base reaction paths. By using the procedure similar to that applied for the synthesis of compounds **3** we have succeeded in the preparation of derivatives of 12*H*-quinoxaline[2,3-*b*]phenoxazine **4** (Scheme 3).

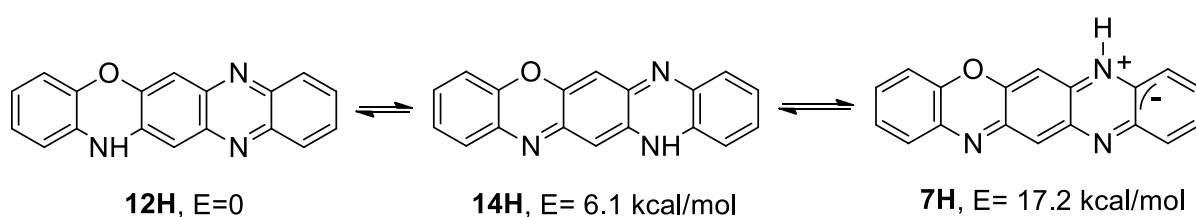


Scheme 3: Synthesis of 12*H*-quinoxaline[2,3-*b*]phenoxazines **4**, **5**.

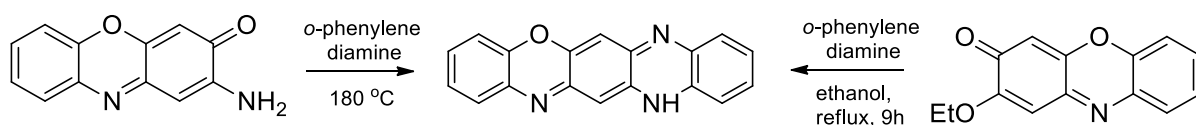
The nitrogen atoms in the oxazine and pyrazine rings of **4** offer three possible positions (N₇, N₁₂, N₁₄) for allocation of a mobile hydrogen atom, therefore, three tautomeric forms are possible for the compounds **4** (Scheme 4), one of which, **7H**, inevitably adopts a bipolar/biradical structure. According to the data of DFT calculations performed at the B3LYP/6-311++G(d,p) approximation (Fig. S6) the energy preferred

tautomer is represented by the **12H** form. The least stable **7H** isomeric structure conforms to a minimum on the corresponding potential energy surface, but its stable wave function corresponds to the electronic state with the so-called “broken symmetry” [17] conclusively indicating at the presence of two unpaired electrons and the singlet biradical form.

In the previous studies of coupling derivatives of 3H-phenoxazin-3-one with *o*-phenylenediamine [10, 11] the preference was given to 14*H*-quinoxaline[2,3-*b*]phenoxazine form (Scheme 5). A series of *N*-aryl derivatives of this form have also been obtained via treatment of *N*-6,8-di-*tert*-butyl-3*H*-phenoxazin-3-ylideneanilines various arylamines in the presence of excessive amounts of trifluoroacetic acid [9].



Scheme 4: Relative stability of the prototropic tautomeric forms of quinoxaline[2,3-*b*]phenoxazine calculated using the DFT B3LYP/6-311++G(d,p) method.



Scheme 5: Preparation of quinoxaline[2,3-*b*]phenoxazines: from 2-amino-[10]- and 2-ethoxy-[11]-3*H*-phenoxazin-3-ones.

The structure of the compounds **4** synthesized in the present work as the derivatives of an earlier unexplored 12*H*-quinoxaline[2,3-*b*]phenoxazine system has been unambiguously established based on the data of COSY, HSQC, heteronuclear multiple bond correlation spectroscopy (HMBC) NMR techniques and ¹⁵NMR spectrum of **4a**

identifying its $^{15}\text{N}(12)$ as a typical pyrrole-type and $^{15}\text{N}(7)$, $^{15}\text{N}(14)$ as pyridine-type nuclei [18, 19] (Fig. S31). The molecular structure of **4a** was also determined using X-ray crystallography (Fig. 4).

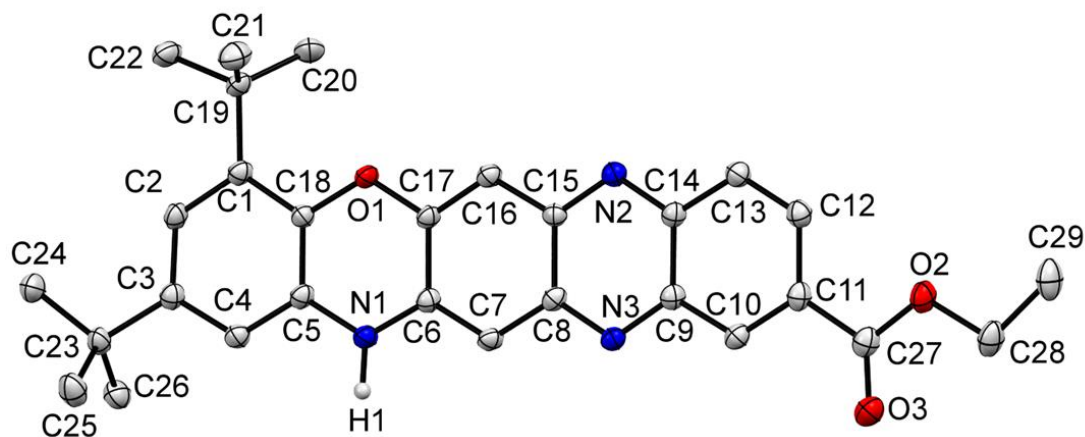
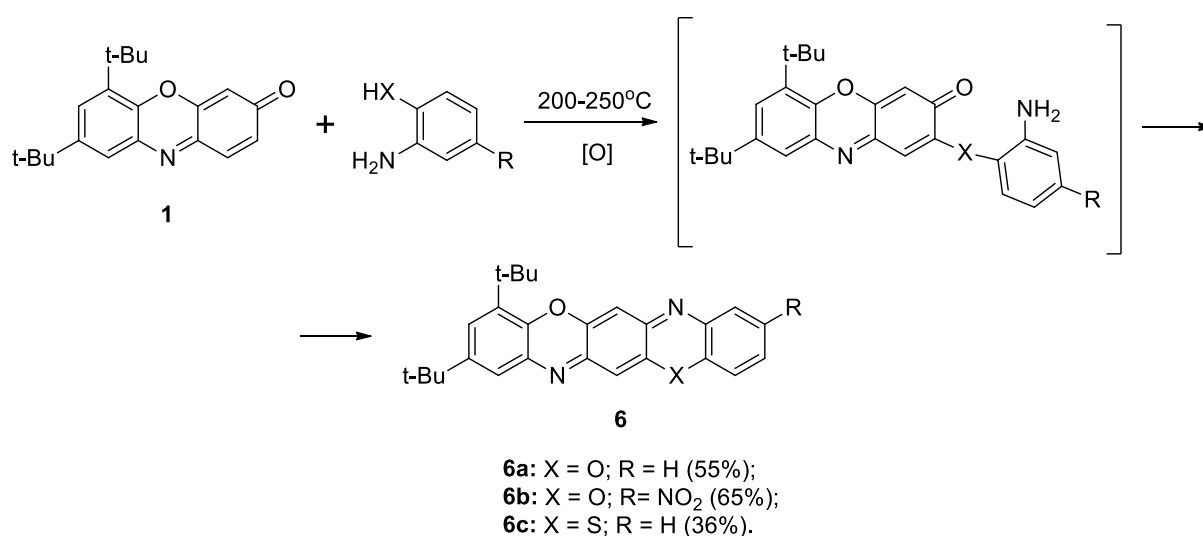


Figure 4: Molecular structure of 10-ethylcarboxylate-2,4-di-*tert*-butyl-14H-quinoxalino[2,3-b]phenoxazine **4c** with the atom numbering scheme. Selected bond distances (Å) and angles: N1-C5 1.390(2), N1-C6 1.365(3), N2-C14 1.363(3), N2-C15 1.336(3), N3-C8 1.338(3), N3-C9 1.356(3), C6-N1-C5 122.13(17), C15-N2-C14 116.88(17), C8-N3-C9 116.66(17). All bond lengths, angles and principal crystallographic parameters are given in SI Tables S5, S6. Hydrogen atoms are omitted for clarity.

We assumed that the scope of the reaction shown in Scheme 3 could be expanded via replacement of one of the amino groups of *o*-phenylenediamine by another strong nucleophilic center. It was earlier found [20] that condensation of 3H-phenoxazin-3-one **1** with various *o*-aminophenols (reflux of DMF solution during 8–10 h) occurring through the intermediate formation of the corresponding imine affords derivatives of benzo[5,6][1,4]oxazino[2,3-b]phenoxazines (triphenodioxazines) **6a,b**. As has been shown in the present work, this reaction can be also successfully performed at the conditions applied for the preparation of 12H-quinoxalino[2,3-b]phenoxazines **4**. The

reaction proceeds readily with *o*-mercaptoaniline to produce a derivative of benzo[5,6][1,4]oxazino[2,3-*b*]phenothiazine system **6c** (Scheme 6).



Scheme 6: Derivatives of triphenodioxazine and oxazinophenothiazine systems via condensation of 3H-phenoxazin-3-one with *o*-amino- and *o*-mercaptophenols.

Electronic absorption spectra of the prepared 12H-quinoxaline[2,3-*b*]phenoxazines **4**, **5** (Table 2, Figs. 5-7, S7-S11) exhibit broad high-intensity longest wavelength absorption bands in the range of 450–550 nm encompassing the strongest emissive part of the solar spectrum. In contrast with non-fluorescent 2-arylaminophenoxazin-3-ones **3**, compounds **4**, **5** display intense fluorescence of their solutions at room temperature (Figs. 5). The excitation spectra of the compounds (Figs. S7-S11) correspond to their longest wavelength absorption bands. The absorption and emission spectra of benzo[5,6][1,4]oxazino[2,3-*b*]phenothiazine **6c** (Fig. 7) are bathochromically (by about 50 nm) shifted relative those of the quinoxaline[2,3-*b*]phenoxazines **5**.

Table 2: UV/vis (λ_{\max} , ϵ) and fluorescence emission (λ_{fl}) data of compounds **4a-c**, **5a,b** and **6c** in toluene. Φ_{fl} – quantum yield of the fluorescence.

Compound	Absorption λ_{\max} , nm ($\epsilon, 10^4 \text{ M}^{-1} \cdot \text{cm}^{-1}$)	Emission λ_{fl} , nm	Φ_{fl}
4a	311 (1.13), 327 ^{sh} (0.83), 380 ^{sh} (0.46), 400 (0.59), 466 (2.36), 486 ^{sh} (2.18)	526, 550 ^{sh}	0.19
4b	307 (1.07), 326 ^{sh} (0.72), 379 ^{sh} (0.45), 401 ^{sh} (0.60), 462 (2.23), 482 (2.12)	519, 542 ^{sh}	0.20
4c	325 (1.32), 339 (1.22), 389 ^{sh} (0.59), 408 (1.47), 484 (2.52), 505 ^{sh} (2.32)	550, 573 ^{sh}	0.13
5a	310 (1.04), 326 ^{sh} (0.78), 379 ^{sh} (0.41), 399 (0.49), 471 (2.29), 486 ^{sh} (2.10)	531, 555 ^{sh}	0.19
5b	314 (1.11), 327 ^{sh} (0.93), 380 ^{sh} (0.46), 400 (0.55), 473 (2.64), 497 (2.50)	531, 555 ^{sh}	0.19
6c	474 ^{sh} (2.13), 502 (4.61), 538 (6.56)	556, 590 ^{sh}	0.35

^{sh}Shoulder

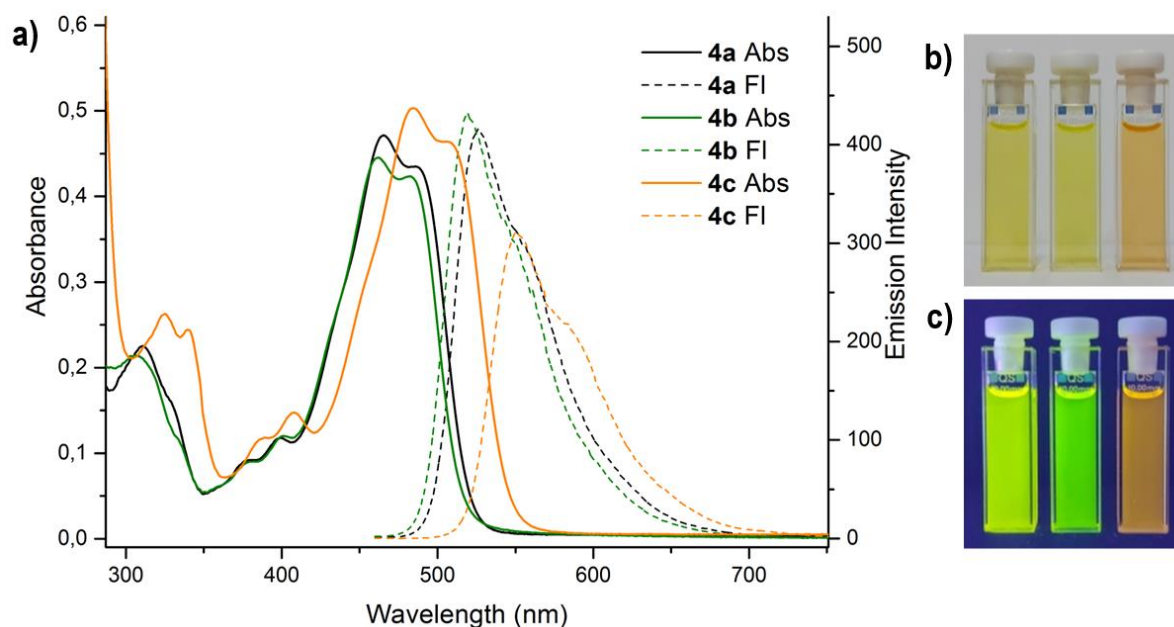


Figure 5: UV/vis (solid lines) and fluorescence emission ($\lambda_{\text{ex}} = 365 \text{ nm}$) (dashed) spectra of compounds **4a-c** (toluene, $C = 2 \cdot 10^{-5} \text{ M}$, $l = 1 \text{ cm}$) (a). Solutions photographs

of compounds **4a-c** in toluene: before irradiation (no emission) (b); during irradiation (photoluminescence, $\lambda_{\text{ex}} = 365 \text{ nm}$) (c) at room temperature.

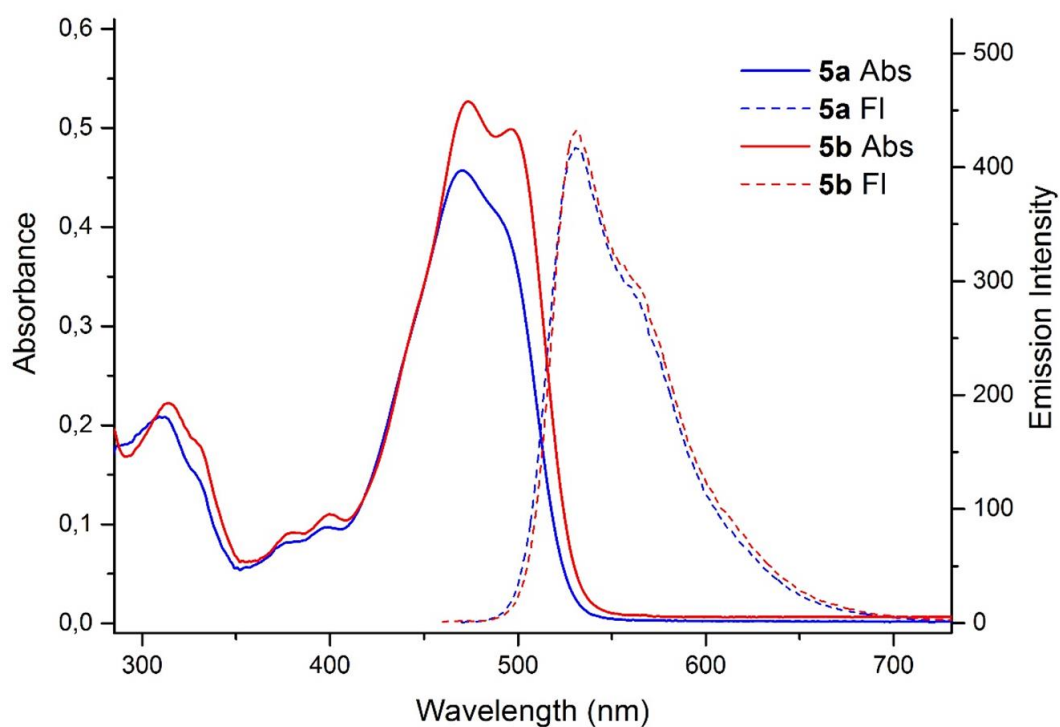


Figure 6: UV/vis (solid lines) and fluorescence emission ($\lambda_{\text{ex}} = 365 \text{ nm}$) (dashed) spectra of **5a** and **5b** (toluene, $C = 2 \cdot 10^{-5} \text{ M}$, $l = 1 \text{ cm}$) at room temperature.

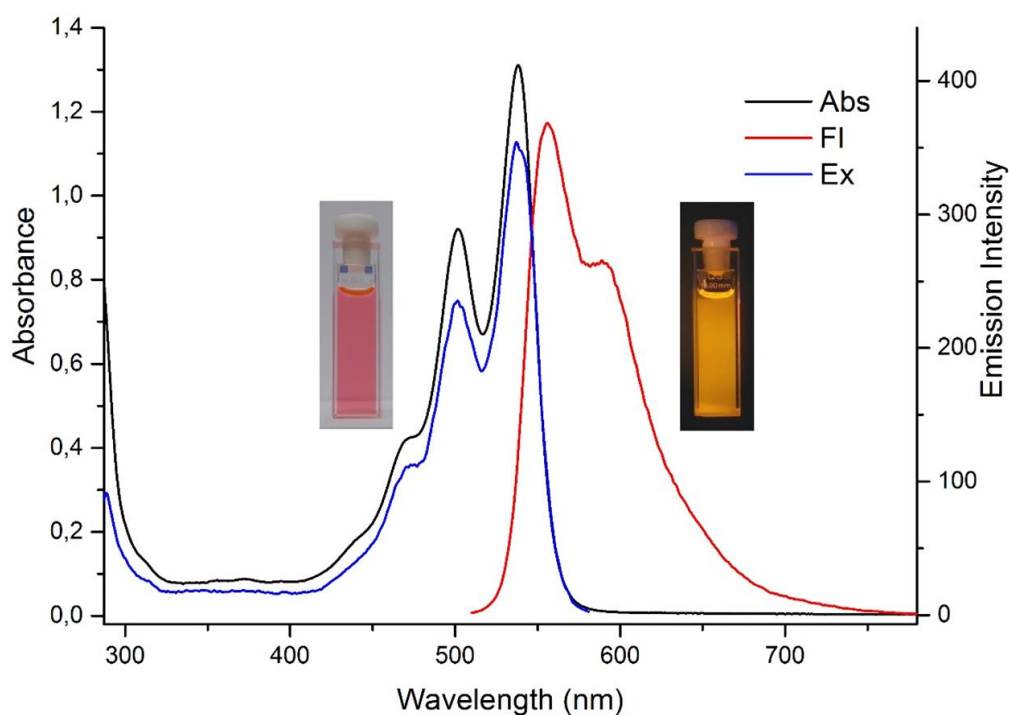


Figure 7: UV/vis, fluorescence emission ($\lambda_{\text{ex}} = 500 \text{ nm}$) and fluorescence excitation ($\lambda_{\text{obs}} = 590 \text{ nm}$) spectra of benzo[5,6][1,4]oxazino[2,3-b]phenothiazine **6c** (toluene, $C = 2 \cdot 10^{-5} \text{ M}$ (Abs), $C = 2 \cdot 10^{-6} \text{ M}$ (Fl, Ex), $l = 1 \text{ cm}$) at room temperature.

Electrochemical behavior of compounds **3a-h**, **4a-c**, **5a,b** and **6c** was studied using cyclic voltammetry (CV). As exemplified by the CV curves (Fig. S12), 2-arylamino-3H-phenoxazin-3-ones **3a-h** manifest two reduction waves at $E_{1/2}^{\text{RED1}} = -1.36 \div -1.69 \text{ V}$ and $E_{1/2}^{\text{RED2}} = -1.85 \div -2.12 \text{ V}$. Oxidation of **3a-f,h** occurs as an irreversible process at $E_{1/2}^{\text{OX}} = 0.81\text{--}1.07 \text{ V}$. For **3g** bearing an amino group the oxidation potential is shifted to $E_{1/2}^{\text{OX}} = 0.25 \text{ V}$. The irreversible, two-wave ($E_{1/2}^{\text{RED1}} = -1.40 \div -1.60 \text{ V}$ and $E_{1/2}^{\text{RED2}} = -1.92 \div -2.45 \text{ V}$) reduction is also characteristic of 2H-quinoxaline[2,3-b]phenoxazines **4a-c** and **5a,b**. In contrast to **4a-c** and **5a,b**, benzo[5,6][1,4]oxazino[2,3-b]phenothiazine **6c** is reversibly reduced at $E_{1/2}^{\text{RED1}} = -1.39 \text{ V}$ to a radical-anion and then undergoes irreversible reduction at $E_{1/2}^{\text{RED2}} = -1.91 \text{ V}$ and irreversible oxidation at $E_{1/2}^{\text{OX}} = 0.48 \text{ V}$. These CV parameters are close to those recorded for triphenodioxazines [20]. The energies of the HOMO and LUMO orbitals assessed on the basis of the CV and electronic absorption spectra data are given in Table 3.

Table 3: CV parameters and calculated energy levels of **3a-h**, **4a-c**, **5a-b** and **6c**.

Compound	CV (vs. Fc ⁺ /Fc)						UV/vis	
	$E_{1/2}^{\text{OX}}$, V	$E_{1/2}^{\text{red1}}$, V	$E_{1/2}^{\text{red2}}$, V	HOMO, eV	LUMO, eV	ΔE , eV	ΔE , eV	LUMO, eV
3a	0.89	-1.41	-1.97	-5.69	-3.39	2.30	2.71	-2.98
3b	0.91	-1.36	-1.90	-5.71	-3.44	2.27	2.77	-2.94
3c	0.83	-1.42	-1.92	-5.63	-3.38	2.25	2.70	-2.93
3d	0.81	-1.36	-1.94	-5.61	-3.44	2.17	2.76	-2.85

3e	1.07	-1.59	-1.91	-5.87	-3.21	2.66	2.71	-3.16
3f	1.05	-1.69	-2.12	-5.85	-3.11	2.74	2.70	-3.15
3g	0.25	-1.54	-1.96	-5.05	-3.26	1.79	2.38	-2.67
3h	0.92	-1.43	-1.85	-5.72	-3.37	2.35	2.73	-2.99
4a	0.86	-1.40	-2.32	-5.66	-3.40	2.26	2.55	-3.11
4b	0.95	-1.60	-2.45	-5.75	-3.20	2.55	2.57	-3.18
4c	0.82	-1.40	-2.15	-5.62	-3.40	2.22	2.46	-3.16
5a	1.10	-1.45	-1.92	-5.9	-3.35	2.55	2.55	-3.35
5b	1.15	-1.48	-2.02	-5.95	-3.32	2.63	2.49	-3.46
6c	0.48	-1.39	-1.91	-5.28	-3.41	1.87	2.30	-2.98

Conclusion

The diverse reactions of derivatives of 3H-phenoxazin-3-one with nucleophilic agents are primarily directed to their *p*-quinone imine fragment [5,13,15]. In the presence of protonic acids the reaction with amines proceeds through the Schiff base formation reaction channel [6], whereas without an acidic catalyst it is driven by the distribution of electronic density (Fig. 1) and the nucleophilic attack is aimed at the most electrophilic C(2) center. With these reasons in mind, we have suggested a convenient procedure for the S_NH reaction of aromatic amines with sterically crowded 6,8-di-*tert*-butyl-3H-phenoxazin-3-one **1** that afforded a series of 2-arylaminophenoxazin-3-ones **3** prepared in 68-93% yields (Scheme 2). Involvement into the process of *o*-amino-, *o*-hydroxy- and *o*-mercapto-substituted anilines allowed activation of both principal reaction channels associated with S_NH and Schiff base reaction paths and led to the formation of derivatives of an earlier unexplored 12*H*-quinoxaline[2,3-*b*]phenoxazine system **4** (Scheme 3) and N,O- and N,S-heteropentacyclic triphenodioxazines and

oxazinophenothiazine **6a-c**. The earlier assignments [10, 11] of the N,O-products of this reaction to derivatives of the 14H-quinoxaline[2,3-*b*]phenoxazines were corrected on the basis on the DFT B3LYP (6–311++G(d,p)) calculations, X-ray structural study and NMR (COSY, HSQC and HMBC) experiments.

Electronic absorption spectra of the heteropentacyclic compounds **4-6** (Table 2, Figs. 5-7) and their electrochemical properties (Table 3) are characteristic of the compounds suitable for testing these as donors for organic solar cells and dye-sensitizers for DSSC [21, 22].

Experimental

All reagents and solvents were purchased from commercial sources (Aldrich) and used without additional purification. The compounds were characterized by ^1H , ^{13}C , ^{15}N NMR (NMR spectra of compounds **3a-h**, **4a-c**, **5a,b** and **6c** are given in SI Figs. S13 – S43), mass-spectroscopy (Figs. S44–S56), IR-, UV/vis absorption and elemental analysis. The NMR spectra were recorded on spectrometers Varian UNITY-300 (300 MHz for ^1H) and Bruker AVANCE-600 (600 MHz for ^1H , 151 MHz for ^{13}C and 60 MHz for ^{15}N) in CDCl_3 solutions, the signals were referred regarding the signals of residual protons of deuterated solvents (7.24 ppm for ^1H), (77.0 ppm for ^{13}C) and (384 ppm for ^{15}N - nitromethane). δ values were measured with precision 0.01 ppm and 0.1 Hz for spin-spin coupling constants J . The assignment of resonance peaks was carried out using two-dimensional correlation techniques COSY (Correlation Spectroscopy ^1H – ^1H), HSQC (Heteronuclear Single Quantum Correlation ^1H – ^{13}C), HMBC (Heteronuclear Multiple Bond Correlation ^1H – ^{13}C , ^1H – ^{15}N). Melting points were determined using a PTP (M) apparatus and were left uncorrected IR spectra were recorded on a Varian Excalibur 3100 FT-IR instrument using the attenuated total

internal reflection technique (ZnSe crystal). UV/vis spectra were recorded for $2 \cdot 10^{-5}$ M toluene solutions with a Varian Cary 100 spectrophotometer. Photoluminescent spectra were recorded for $2 \cdot 10^{-5}$ M (compounds **4a-c** and **5a,b**) and for $2 \cdot 10^{-6}$ M (compound **6c**) toluene solutions with a Varian Cary Eclipse fluorescence spectrophotometer. UV/Vis and fluorescence spectra were recorded using standard 1 cm quartz cells at room temperature. Toluene of the spectroscopic grade (Aldrich) was used to prepare solutions. Fluorescence quantum yields determined relative to quinine bisulfate in 0.05 M H₂SO₄ as standard ($\Phi_F = 0.52$; excitation at 365 nm) (compounds **4a-c** and **5a,b**) [23] and cresyl violet perchlorate in ethanol ($\Phi_F = 0.54$; excitation at 510 nm) (compound **6c**) [24]. Mass spectrometric analysis was performed on a Bruker UHR-TOF Maxis™ Impact (resolving power (FWHM) of 40000 at m/z 1222) (electrospray ionization). The cyclic voltammetry of compounds **3a-h**, **4a-c**, **5a,b** and **6c** was measured with the use of three-electrode configuration (glassy-carbon working electrode, Pt counter electrode, Ag/Ag⁺ reference electrode (0.01 M AgNO₃ in CH₃CN)) in CH₂Cl₂ (**3a-h**), CH₃CN (**4a-c**, **5a,b** and **6c**) and potentiostat-galvanostat Elins P-45X. The data collection has been performed on an Agilent SuperNova diffractometer using microfocus X-ray source with copper anode (CuK α $\lambda = 1.54184$) and Atlas S2 CCD detector. The diffraction data of **3c-e**, **4c** and **6b** were obtained at 100 K. Crystals of **4c** were obtained in the form of solvate with molecules of isopropanol and water. Protons on heteroatoms were localized from difference Fourier synthesis and refined with isotropic thermal parameters. The collection of reflexes, determination and refinement of unit cell parameters were performed by using the specialized CrysAlisPro 1.171.38.41 software suite [25]. The structures were solved by using ShelXT program [26], structure refinement was also performed with ShelXL program [27]. Molecular graphics were rendered and prepared for publication with the Olex2 version 1.3.0 software suite [28]. The complete X-ray diffraction datasets were deposited at the

Cambridge Crystallographic Data Center (deposit CCDC 2292841, 2292840, 2292847, 2308520, 2292848) (SI Tables S1–S8). The density functional theory (DFT) [29] calculations were performed using the Gaussian 16 program package [30] with the B3LYP functional [31] and 6–311++G(d,p) basis set. The structures discussed in the work, which correspond to minima on the potential energy surface (PES) and states with “broken symmetry” (BS) [17], were found through complete optimization of the geometry without imposing symmetry restrictions, followed by checking the stability of the DFT wave function. Graphic images of molecular structures presented in Figures 1 and S6 were obtained using the ChemCraft program [32].

Synthesis

General procedure for the synthesis of compounds 3a-h

309 mg (1 mmol) of 6,8-di-*tert*-butyl-3H-phenoxazin-3-one **1** powder was mixed with 3 mmol of the corresponding amine powder, placed in a round-bottom flask and heated in a glycerin bath for 30 minutes at a temperature of 250-270 °C, stirring melt with a spatula every 10 min. For compounds **3a-h**, the reaction mixture was separated by column chromatography (carrier Al₂O₃, eluent toluene), and the resulting fraction was recrystallized from diethyl ether.

6,8-di-*tert*-butyl-2-(phenylamino)-3H-phenoxazin-3-one 3a

Dark orange solid with m.p. 145-147 °C. Yield 80% (320 mg). R_f ~ 0.70. IR (neat, cm⁻¹): 3269 (N-H), 2950 (t-Bu), 2903 (t-Bu), 2863 (t-Bu), 1566 (C=O), 1519 (C=N), 1266 (C-N), 1239 (C-N), 1182 (C-O), 1159 (C-O). ¹H NMR (600 MHz, CDCl₃) δ 7.71 (s, 1H), 7.63 (d, *J* = 2.1 Hz, 1H), 7.49 (d, *J* = 2.1 Hz, 1H), 7.37 (t, *J* = 7.8 Hz, 2H), 7.33 (d, *J* = 7.8 Hz, 2H), 7.12 (t, *J* = 7.8 Hz, 1H), 7.00 (s, 1H), 6.52 (s, 1H), 1.51 (s, 9H), 1.36 (s, 9H). ¹³C NMR (151 MHz, CDCl₃) δ 180.08, 149.34, 147.85, 147.53, 141.98, 139.45,

138.94, 136.75, 134.20, 129.57, 125.33, 124.39, 123.81, 121.39, 103.20, 99.48, 35.17, 34.87, 31.40, 30.08. HRMS (ESI) m/z: [M+H]⁺ Calcd. for C₂₆H₂₉N₂O₂ 401.2224; Found 401.2229.

6,8-di-tert-butyl-2-((2-iodophenyl)amino)-3H-phenoxazin-3-one 3b

Orange needle crystals with m.p. 170-173 °C. Yield 82% (431 mg). R_f ~ 0.70. IR (neat, cm⁻¹): 3243 (N-H), 2961 (t-Bu), 2902 (t-Bu), 2868 (t-Bu), 1580 (C=O), 1529 (C=N), 1264 (C-N), 1208 (C-N), 1162 (C-O), 1150 (C-O). ¹H NMR (600 MHz, CDCl₃) δ 7.89 (d, *J* = 7.9, 1H), 7.78 (s, 1H), 7.62 (d, *J* = 2.3 Hz, 1H), 7.55 (d, *J* = 7.9 Hz, 1H), 7.50 (d, *J* = 2.3 Hz, 1H), 7.38 (t, *J* = 7.9 Hz, 1H), 6.89 (t, *J* = 7.9 Hz, 1H), 6.85 (s, 1H), 6.55 (s, 1H), 1.51 (s, 9H), 1.36 (s, 9H). ¹³C NMR (151 MHz, CDCl₃) δ 179.74, 149.28, 147.88, 147.45, 141.81, 140.03, 139.86, 136.78, 134.08, 129.21, 126.17, 125.60, 123.83, 122.13, 103.33, 100.05, 93.67, 35.15, 34.84, 31.36, 30.03. HRMS (ESI) m/z: [M+H]⁺ Calcd. for C₂₆H₂₈IN₂O₂ 527.1132; Found 527.1135.

6,8-di-tert-butyl-2-((3-methoxyphenyl)amino)-3H-phenoxazin-3-one 3c

Brown needle crystals with m.p. 163-165 °C. Yield 87% (374 mg). R_f ~ 0.70. IR (neat, cm⁻¹): 3316 (N-H), 2952 (t-Bu), 2904 (t-Bu), 2868 (t-Bu), 1580 (C=O), 1523 (C=N), 1256 (C-N), 1238 (C-N), 1174 (C-O), 1143 (C-O). ¹H NMR (600 MHz, CDCl₃) δ 7.69 (s, 1H), 7.64 (d, *J* = 2.3 Hz, 1H), 7.49 (d, *J* = 2.3 Hz, 1H), 7.28 (t, *J* = 8.1 Hz, 1H), 7.03 (s, 1H), 6.94 (dd, *J* = 8.1, 2.2 Hz, 1H), 6.85 (t, *J* = 2.2 Hz, 1H), 6.68 (dd, *J* = 8.1, 2.2 Hz, 1H), 6.51 (s, 1H), 3.81 (s, 3H), 1.51 (s, 9H), 1.36 (s, 9H). ¹³C NMR (151 MHz, CDCl₃) δ 180.03, 160.69, 149.29, 147.83, 147.48, 141.80, 140.10, 139.41, 136.71, 134.18, 130.27, 125.34, 123.78, 113.63, 109.73, 107.41, 103.14, 99.94, 55.36, 35.13, 34.83, 31.36, 30.03. HRMS (ESI) m/z: [M+H]⁺ Calcd. for C₂₇H₃₁N₂O₃ 431.2329; Found 431.2339.

6,8-di-tert-butyl-2-((3-chlorophenyl)amino)-3H-phenoxazin-3-one 3d

Brown needle crystals with m.p. 171-174 °C. Yield 79% (344 mg). R_f ~ 0.70. IR (neat, cm⁻¹): 3274 (N-H), 2952 (t-Bu), 2905 (t-Bu), 2866 (t-Bu), 1574 (C=O), 1519 (C=N), 1264 (C-N), 1239 (C-N), 1207 (C-O), 1157 (C-O). ¹H NMR (600 MHz, CDCl₃) δ 7.72 (s, 1H), 7.65 (d, *J* = 2.3 Hz, 1H), 7.51 (d, *J* = 2.3 Hz, 1H), 7.34 (t, *J* = 2.0 Hz, 1H), 7.29 (t, *J* = 8.0 Hz, 1H), 7.20 (dd, *J* = 8.0, 2.0 Hz, 1H), 7.09 (dd, *J* = 8.0, 2.0 Hz, 1H), 7.01 (s, 1H), 6.52 (s, 1H), 1.51 (s, 9H), 1.37 (s, 9H). ¹³C NMR (151 MHz, CDCl₃) δ 179.69, 149.26, 147.97, 147.29, 141.27, 140.25, 139.46, 136.76, 135.25, 134.09, 130.49, 125.71, 124.21, 123.86, 120.86, 119.19, 103.15, 100.35, 35.12, 34.83, 31.32, 30.00. HRMS (ESI) m/z: [M+H]⁺ Calcd. for C₂₆H₂₈ClN₂O₂ 435.1834; Found 435.1837.

6,8-di-tert-butyl-2-((4-nitrophenyl)amino)-3H-phenoxazin-3-one 3e

Dark orange powder with m.p. 180-183 °C. Yield 88% (391 mg). R_f ~ 0.70. IR (neat, cm⁻¹): 3250 (N-H), 2953 (t-Bu), 2904 (t-Bu), 2866 (t-Bu), 1637 (C=O), 1582 (C=N), 1574 (N=O), 1269 (C-N), 1240 (C-N), 1155 (C-O), 1111 (C-O). ¹H NMR (600 MHz, CDCl₃) δ 8.24 (d, *J* = 8.6 Hz, 2H), 8.15 (s, 1H), 7.67 (s, 1H), 7.56 (s, 1H), 7.41 (d, *J* = 8.6 Hz, 2H), 7.22 (s, 1H), 6.55 (s, 1H), 1.51 (s, 9H), 1.37 (s, 9H). ¹³C NMR (151 MHz, CDCl₃) δ 179.39, 149.32, 148.37, 146.97, 145.27, 142.72, 139.75, 139.71, 136.98, 134.15, 126.73, 125.73, 124.24, 118.89, 103.50, 103.33, 35.22, 34.92, 31.35, 30.05. HRMS (ESI) m/z: [M-H]⁻ calcd for C₂₆H₂₆N₂O₂ 444.1929; found 444.1933.

6,8-di-tert-butyl-2-((2-nitrophenyl)amino)-3H-phenoxazin-3-one 3f

Orange needle crystals with m.p. 178-180 °C. Yield 93% (414 mg). R_f ~ 0.70. IR (neat, cm⁻¹): 3221 (N-H), 2997 (t-Bu), 2961 (t-Bu), 2869 (t-Bu), 1589 (C=O), 1572 (N=O), 1509 (C=N), 1262 (C-N), 1241 (C-N), 1153 (C-O), 1111 (C-O). ¹H NMR (600 MHz, CDCl₃) δ 10.19 (s, 1H), 8.23 (d, *J* = 8.4, 1H), 7.86 (d, *J* = 8.4 Hz, 1H), 7.64 (d, *J* = 2.3 Hz, 1H), 7.62 (t, *J* = 8.4 Hz, 1H), 7.54 (d, *J* = 2.3 Hz, 1H), 7.13 (t, *J* = 8.4 Hz, 1H), 6.56

(s, 1H), 1.51 (s, 9H), 1.36 (s, 9H). ^{13}C NMR (151 MHz, CDCl_3) δ 179.46, 149.08, 148.10, 147.26, 140.27, 139.73, 138.71, 136.94, 136.08, 135.04, 134.00, 126.91, 126.51, 124.15, 122.29, 120.56, 104.37, 103.76, 35.18, 34.86, 31.33, 30.01. HRMS (ESI) m/z: $[\text{M}-\text{Na}]^+$ calcd for $\text{C}_{26}\text{H}_{27}\text{N}_3\text{NaO}_4$ 468.1894; found 468.1887.

2-((4-aminophenyl)amino)-6,8-di-tert-butyl-3H-phenoxazin-3-one 3g

Dark green powder with m.p. 156-158 °C. Yield 68% (282 mg). Rf ~ 0.70. IR (neat, cm^{-1}): 3410 (N-H), 3262 (N-H), 3208 (N-H), 2953 (t-Bu), 2902 (t-Bu), 2867 (t-Bu), 1637 (C=O), 1573 (C=N), 1265 (C-N), 1240 (C-N), 1182 (C-O), 1155 (C-O). ^1H NMR (600 MHz, CDCl_3) δ 7.60 (d, $J = 2.3$ Hz, 1H), 7.49 (s, 1H), 7.45 (d, $J = 2.3$ Hz, 1H), 7.11 (d, $J = 8.6$ Hz, 2H), 6.74 (s, 1H), 6.69 (d, $J = 8.6$ Hz, 2H), 6.48 (s, 1H), 3.69 (s, 2H), 1.50 (s, 9H), 1.35 (s, 9H). ^{13}C NMR (151 MHz, CDCl_3) δ 180.22, 149.42, 147.63, 147.44, 143.86, 143.14, 139.24, 136.60, 134.18, 129.63, 124.71, 123.87, 123.50, 115.82, 103.04, 97.89, 35.08, 34.78, 31.34, 30.01. HRMS (ESI) m/z: $[\text{M}+\text{H}]^+$ Calcd. for $\text{C}_{26}\text{H}_{30}\text{N}_3\text{O}_2$ 416.2342; Found 416.2333.

methyl 4-((6,8-di-tert-butyl-3-oxo-3H-phenoxazin-2-yl)amino)benzoate 3h

Red-brown powder with m.p. 174-177 °C. Yield 81% (371 mg). Rf ~ 0.70. IR (neat, cm^{-1}): 3264 (N-H), 2950 (t-Bu), 2902 (t-Bu), 2869 (t-Bu), 1713 (C=O), 1580 (C=O), 1531 (C=N), 1280 (C-N), 1265 (C-N), 1182 (C-O), 1156 (C-O), 1111 (C-O). ^1H NMR (600 MHz, CDCl_3) δ 8.04 (d, $J = 8.7$ Hz, 2H), 7.95 (s, 1H), 7.66 (d, $J = 2.3$ Hz, 1H), 7.52 (d, $J = 2.3$ Hz, 1H), 7.36 (d, $J = 8.7$ Hz, 2H), 7.16 (s, 1H), 6.53 (s, 1H), 3.90 (s, 3H), 1.51 (s, 9H), 1.37 (s, 9H). ^{13}C NMR (151 MHz, CDCl_3) δ 179.68, 166.39, 149.26, 148.06, 147.26, 143.35, 140.44, 139.55, 136.82, 134.14, 131.31, 126.00, 125.01, 124.02, 119.22, 103.23, 101.81, 51.98, 35.15, 34.86, 31.34, 30.02. HRMS (ESI) m/z: $[\text{M}-\text{H}]^-$ Calcd. for $\text{C}_{28}\text{H}_{29}\text{N}_2\text{O}_4$ 457.2133; Found 457.2131.

General procedure for the synthesis of compounds 4a-c

309 mg (1 mmol) of 6,8-di-*tert*-butyl-3H-phenoxazin-3-one **1** powder was mixed with 3 mmol of the corresponding *o*-phenylenediamine powder, placed in a round-bottom flask and heated in a glycerin bath for 30 minutes at a temperature of 200-250 °C, stirring the melt with a spatula every 10 min. The reaction mixture was separated by column chromatography (Al₂O₃ carrier, eluent dichloromethane and isopropanol (*l* = 40 cm, *d* = 15 mm)). The resulting fraction was recrystallized from isopropanol.

2,4-di-*tert*-butyl-14H-quinoxalino[2,3-*b*]phenoxazine 4a

Red powder with m.p. > 260 °C. Yield 93% (369 mg). R_f ~ 0.45. IR (neat, cm⁻¹): 3264 (N-H), 3087 (t-Bu), 2949 (t-Bu), 2902 (t-Bu), 2865 (t-Bu), 1618 (C=N), 1593 (C=N), 1235 (C-N), 1211 (C-N), 1179 (C-N), 1139 (C-O), 1113 (C-O). ¹H NMR (600 MHz, CDCl₃) δ 8.01 (s, 1H), 7.96 (d, *J* = 7.8 Hz, 1H), 7.87 (d, *J* = 7.8 Hz, 1H), 7.48 (t, *J* = 7.8 Hz, 2H), 7.47 (t, *J* = 7.8 Hz, 2H), 7.26 (s, 1H), 6.85 (s, 1H), 6.74 (d, *J* = 2.4 Hz, 1H), 6.42 (d, *J* = 2.4 Hz, 1H), 1.46 (s, 9H), 1.13 (s, 9H). ¹³C NMR (151 MHz, CDCl₃) δ 148.97, 146.46, 144.11, 143.58, 142.19, 141.67, 138.09, 136.94, 136.53, 129.10, 128.98, 128.02, 127.80, 127.28, 117.04, 109.69, 109.64, 102.35, 34.93, 34.38, 31.20, 29.98. ¹⁵N NMR (60 MHz, CDCl₃) δ 314.85, 296.56, 92.79. HRMS (ESI) *m/z*: [M+H]⁺ Calcd. for C₂₆H₂₈N₃O 398.2227; Found 398.2218.

2,4-di-*tert*-butyl-9,10-dimethyl-14H-quinoxalino[2,3-*b*]phenoxazine 4b

Red powder with m.p. > 260 °C. Yield 69% (293 mg). R_f ~ 0.48. IR (neat, cm⁻¹): 3245 (N-H), 2952 (t-Bu), 2867 (t-Bu), 1615 (C=N), 1592 (C=N), 1238 (C-N), 1212 (C-N), 1168 (C-N), 1110 (C-O), 1032 (C-O). ¹H NMR (600 MHz, CDCl₃) δ 7.72 (s, 1H), 7.65 (s, 1H), 7.25 (s, 1H), 6.79 (s, 1H), 6.74 (d, *J* = 1.9 Hz, 1H), 6.42 (d, *J* = 1.9 Hz, 1H), 2.37 (s, 3H), 2.36 (s, 3H), 1.46 (s, 9H), 1.15 (s, 9H). ¹³C NMR (151 MHz, CDCl₃) δ 148.36, 146.23, 143.42, 142.80, 141.43, 140.93, 140.04, 138.90, 138.12, 136.90,

135.83, 127.63, 127.61, 126.71, 116.87, 109.79, 109.48, 102.86, 34.91, 34.36, 31.20, 29.95, 20.35, 20.26. HRMS (ESI) m/z: [M+H]⁺ Calcd. for C₂₈H₃₂N₃O 426.2540; Found 426.2534.

ethyl 2,4-di-tert-butyl-14H-quinoxalino[2,3-b]phenoxazine-10-carboxylate 4c

Violet powder with m.p. > 260 °C. Yield 63% (295 mg). R_f ~ 0.54. IR (neat, cm⁻¹): 3330 (N-H), 2952 (t-Bu), 2902 (t-Bu), 2866 (t-Bu), 1701 (C=O), 1646 (C=N), 1592 (C=N), 1261 (C-N), 1233 (C-N), 1196 (C-N), 1174 (C-O), 1088 (C-O). ¹H NMR (600 MHz, CDCl₃) (600 MHz, CDCl₃) δ 8.64 (s, 1H), 8.11 (d, *J* = 8.8 Hz, 1H), 7.98 (d, *J* = 8.8 Hz, 1H), 7.65 – 7.45 (m, 2H), 6.84 (s, 1H), 6.80 (s, 1H), 6.46 (s, 1H), 4.36 (q, *J* = 7.1 Hz, 2H), 1.44 (s, 9H), 1.35 (t, *J* = 7.1 Hz, 3H), 1.18 (s, 9H). ¹³C NMR (151 MHz, CDCl₃) δ 166.08, 150.01, 146.82, 145.07, 144.82, 143.39, 141.54, 138.03, 137.21, 136.64, 131.11, 130.57, 129.04, 127.32, 126.97, 117.49, 109.79, 109.55, 102.72, 61.35, 34.96, 34.49, 31.25, 29.96, 14.25. HRMS (ESI) m/z: [M+H]⁺ Calcd. for C₂₉H₃₁N₃O₃ 470.2438; Found 470.2444.

General procedure for the synthesis of compounds 5a,b

100 mg (0.25 mmol) of 2,4-di-*tert*-butyl-14H-quinoxalino[2,3-*b*]phenoxazine in 15 ml of acetone was added to 40 mg (1 mmol) of sodium hydroxide. After the solution took on an intense blue color, 0.1 ml (1.6 mmol) methyl iodide was added for **5a** or 254 mg (1 mmol) 1-iodononane for **5b** and stirred at room temperature for 4 hours. The reaction mixture was filtered, and the mother liquor was recrystallized from acetone.

2,4-di-tert-butyl-14-methyl-14H-quinoxalino[2,3-b]phenoxazine 5a

Red powder with m.p. 232-235 °C. Yield 97% (398 mg). R_f ~ 0.80. IR (neat, cm⁻¹): 2950 (t-Bu), 2924 (t-Bu), 2860 (t-Bu), 1579 (C=N), 1563 (C=N), 1342 (C-N), 1301 (C-N), 1236 (C-N), 1222 (C-N), 1128 (C-O), 1070 (C-O). ¹H NMR (600 MHz, CDCl₃) δ 8.01 (d, *J* = 8.1 Hz, 1H), 7.98 (d, *J* = 8.1 Hz, 1H), 7.63 (t, *J* = 8.1 Hz, 1H), 7.60 (t, *J* =

8.1 Hz, 1H), 7.34 (s, 1H), 6.94 (s, 1H), 6.93 (d, $J = 2.1$, 1H), 6.71 (d, $J = 2.1$, 1H), 3.37 (s, 3H), 1.46 (s, 9H), 1.31 (s, 9H). ^{13}C NMR (151 MHz, CDCl_3) δ 150.45, 146.30, 144.48, 143.17, 142.70, 141.90, 140.04, 139.19, 136.92, 130.84, 129.07, 128.90, 128.49, 128.31, 117.35, 109.17, 108.55, 103.54, 34.97, 34.83, 32.45, 31.45, 30.03. ^{15}N NMR (60 MHz, CDCl_3) δ 311.64, 305.64, 83.69. HRMS (ESI) m/z : $[\text{M}+\text{H}]^+$ Calcd. for $\text{C}_{27}\text{H}_{30}\text{N}_3\text{O}$ 412.2383; Found 412.2389.

2,4-di-tert-butyl-14-nonyl-14H-quinoxalino[2,3-b]phenoxazine 5b

Red powder with m.p. 154-157 °C. Yield 91% (476 mg). $R_f \sim 0.73$. IR (neat, cm^{-1}): 2948 (t-Bu), 2927 (t-Bu), 2863 (t-Bu), 1582 (C=N), 1568 (C=N), 1346 (C-N), 1299 (C-N), 1231 (C-N), 1220 (C-N), 1128 (C-O), 1083 (C-O). ^1H NMR (600 MHz, CDCl_3) δ 7.98 (d, $J = 8.1$ Hz, 1H), 7.97 (d, $J = 8.1$ Hz, 1H), 7.63 (t, $J = 8.1$ Hz, 1H), 7.59 (t, $J = 8.1$ Hz, 1H), 7.29 (s, 1H), 6.91 (s, 1H), 6.90 (d, $J = 2.1$, 1H), 6.70 (d, $J = 2.1$, 1H), 3.79 (t, $J = 8.3$, 2H), 1.85 (qvin, $J = 7.6$, 2H), 1.53 (m, 2H), 1.50 (m, 2H), 1.45 (s, 9H), 1.42 (m 2H), 1.35 (m, 2H), 1.32 (m, 2H), 1.31 (s, 9H), 1.28 (m, 2H), 0.89 (t, $J = 7.0$, 3H). ^{13}C NMR (151 MHz, CDCl_3) δ 149.87, 146.04, 144.76, 143.29, 142.74, 141.90, 139.44, 137.50, 136.82, 129.19, 129.02, 128.89, 128.34, 128.17, 117.25, 108.99, 108.41, 102.76, 45.61, 34.99, 34.77, 31.83, 31.41, 29.99, 29.54, 29.39, 29.21, 26.97, 24.74, 22.65, 14.07. ^{15}N NMR (60 MHz, CDCl_3) δ 310.36, 303.85, 96.38. HRMS (ESI) m/z : $[\text{M}+\text{H}]^+$ Calcd. for $\text{C}_{35}\text{H}_{46}\text{N}_3\text{O}$ 524.3635; Found 524.3640.

General procedure for the synthesis of compounds 6a,b

309 mg (1 mmol) of 6,8-di-*tert*-butyl-3H-phenoxazin-3-one **1** powder was mixed with 3 mmol of the corresponding *o*-aminophenol powder, placed in a round-bottom flask and heated in a glycerin bath for 30 minutes at a temperature of 250-270 °C, stirring the melt with a spatula every 10 minutes. The structure of the obtained products **6a,b** corresponded to those previously described [20].

2,4-di-tert-butylbenzo[5,6][1,4]oxazino[2,3-b]phenoxazine 6a

The reaction mixture was separated by column chromatography on Al₂O₃, toluene, Rf ~ 0.70. Red powder. Yield 55% (219 mg). M.p. 228–229 °C.

2,4-di-tert-butyl-9-nitrobenzo[5,6][1,4]oxazino[2,3-b]phenoxazine 6b

The reaction mixture was separated by column chromatography on Al₂O₃, toluene, Rf ~ 0.75. Red powder. Yield 65% (288 mg). M.p. > 260 °C.

2,4-di-tert-butylbenzo[5,6][1,4]oxazino[2,3-b]phenothiazine 6c

309 mg (1 mmol) of 6,8-di-tert-butyl-3H-phenoxazin-3-one **1** powder was mixed with 375 mg (3 mmol) of 2-aminobenzenethiol powder, placed in a round-bottom flask and heated in a glycerin bath for 30 minutes at a temperature of 200-250 °C, stirring melt with a spatula every 10 minutes. The reaction mixture was separated by column chromatography (Al₂O₃ carrier, eluent dichloromethane (*l* = 40 cm, *d* = 15 mm)). Violet powder with m.p. 211-215 °C. Yield 36% (149 mg). Rf ~ 0.80. IR (neat, cm⁻¹): 2943 (t-Bu), 2867 (t-Bu), 1569 (C=N), 1516 (C=N), 1333 (C-N), 1310 (C-N), 1267 (C-N), 1241 (C-N), 1141 (C-O), 1122 (C-O), 569 (C-S). ¹H NMR (600 MHz, CDCl₃) δ 7.43 (d, *J* = 7.8 Hz, 1H), 7.28 (d, *J* = 2.3 Hz, 1H), 7.24 (d, *J* = 2.3 Hz, 1H), 7.23 – 7.19 (m, 1H), 7.13 – 7.07 (m, 2H), 6.76 (s, 1H), 6.57 (s, 1H), 1.43 (s, 9H), 1.30 (s, 9H). ¹³C NMR (151 MHz, CDCl₃) δ 151.00, 149.15, 148.33, 147.26, 141.26, 141.17, 136.09, 135.39, 132.07, 131.27, 127.73, 127.70, 124.78, 124.71, 123.75, 121.77, 118.80, 108.44, 34.90, 34.62, 31.30, 29.89. HRMS (ESI) *m/z*: [M+H]⁺ Calcd. for C₂₆H₂₇N₂OS 415.1839; Found 415.1845.

Supporting Information

Supporting information to this article can be found online at

Funding

This work has been financially supported by the Russian Science Foundation (project no. 19-13-00022, <https://rscf.ru/project/19-13-00022/>).

References

1. Zorrilla, J. G.; Rial, C.; Cabrera, D.; Molinillo, J. M. G.; Varela, R. M.; Macías, F. A. *Molecules*, **2021**, *26*, 3453. DOI: 10.3390/molecules26113453
2. Sadhu, C.; Mitra, A. K. *Mol Diversity*. Springer. **2023**. DOI: 10.1007/s11030-023-10619-5
3. Diepolder, F. *Chem Ber*, **1902**, *35*, 2816–2822. DOI: 10.1002/cber.19020350360
4. Podder, N.; Mandal, S. *New J. Chem.*, **2020**, *44*, 12793-12805. DOI: 10.1039/d0nj02558e
5. Abakumov, G. A.; Druzhkov, N. O.; Kurskii, Yu. A.; Abakumova, L. G.; Shavyrin, A. S.; Fukin, G. K. *Russ. Chem. Bull.*, **2005**, *54*, 2571–2577. DOI: 10.1007/s11172-006-0157-7
6. Ivakhnenko, E. P.; Knyazev, P. A.; Kovalenko, A. A.; Romanenko, G. V.; Revinskii, Yu. V.; Starikov, A. G.; Minkin, V. I. *Tetr. Lett.*, **2020**, *61*, 151429. DOI: 10.1016/j.tetlet.2019.151429
7. Kulszewicz-Bajer, I. J. *Mater. Chem. C.*, **2022**, 12377-12391. DOI: 10.1039/D2TC02270B
8. Lv, L.; Luo, W.; Diao, Q. *Spectrochim. Acta Part A.*, **2021**, *246*, 118959. DOI: 10.1016/j.saa.2020.118959
9. Ivakhnenko, E. P.; Knyazev, P. A.; Omelichkin, N. I.; Makarova, N. I.; Starikov, A. G.; Aleksandrov, A. E.; Ezhov, A. V.; Tameev, A. R.; Demidov, O. P.; Minkin, V. I. *Dyes Pigments*, **2022**, *197*, 109848. DOI: 10.1016/j.dyepig.2021.109848

10. Martinek, M.; Kotoucek, M.; Ruzicka, E. *Monatsh. Chem.*, **1967**, *98*, 1532-1536.
DOI: 10.1007/bf00909022
11. Afanas'eva, G. B.; Postovskii, I. Ya.; Viktorova, T. S. *Chem. Geterocycl. Compd.*, **1978**, *14*, 966-968. DOI: 10.1007/bf00509550
12. Ivakhnenko, E. P.; Romanenko, G. V.; Kovalenko, A. A.; Revinskii, Yu. V.; Knyazev, P. A.; Kuzmin, V. A.; Minkin, V. I. *Dyes Pigments*, **2018**, *150*, 99-104. DOI: 10.1016/j.dyepig.2017.11.009
13. Yang, J.; Martien, A.; Cohen Stuart, M. A.; Kamperman, M. *Chem. Soc. Rev.*, **2014**, *43*, 8271-8298. DOI: 10.1039/c4cs00185k
14. Vasu, D.; Leitch, J. A.; Dixon, D. J. *Tetrahedron*, **2019**, *75*, 130726. DOI: 10.1016/j.tet.2019.130726
15. Kutryev, A. A. *Tetrahedron*, **1991**, *47*, 8043-8065. DOI: 10.1016/S0040-4020(01)91002-6
16. Viktorova, T. S.; Afanas'eva, G. B.; Postovskii, I. Ya.; Ivanova, L. V. *Chem. Geterocycl. Compd.*, **1974**, 1196-1199.
17. Noodleman, L. *J. Chem. Phys.*, **1981**, *74*, 5737-5743. DOI: 10.1063/1.440939
18. Świdorski, G.; Wojtulewski, S.; Kalinowska, M.; Świsłocka, R.; Lewandowski, W. *J. Mol. Str.*, **2011**, *993*, 448-458. DOI: 10.1016/j.molstruc.2011.01.026
19. Pearse, G. A.; Raithby, P. R.; Lewis, J. *Polyhedron*, **1989**, *8*, 301-304. DOI: 10.1016/S0277-5387(00)80418-0
20. Ivakhnenko, E. P.; Romanenko, G. V.; Makarova, N. I.; Kovalenko, A. A.; Knyazev, P. A.; Rostovtseva, I. A.; Starikov, A. G.; Minkin, V. I. *Dyes Pigments*, **2020**, *176*, 108174. DOI: 10.1016/j.dyepig.2019.108174
21. Yahya, M.; Bouziani, A.; Ocak, C.; Seferoglu, Z.; Sillanpa, M. *Dyes Pigments*, **2021**; *192*, 109227. DOI: 10.1016/j.dyepig.2021.109227.

22. Li, Y.; Huang, W.; Zhao, D.; Wang, L.; Jiao, Z.; Huang, Q.; Wang, P.; Sun, M.; Yuan, G. *Molecules*. **2022**; *27*, 1800. DOI: 10.3390/molecules27061800
23. Meech, S. R.; Phillips, D. *J. Photochem.*, **1983**, *23*, 193-217.
24. Magde, D.; Brannon, J. H.; Cremers, T. L.; Olmsted, J. *J. Phys. Chem.*, **1979**, *83*, 696-699.
25. CrysAlisPro, version 1.171.38.41. Rigaku oxford diffraction. <https://www.rigaku.com/en/products/smc/crysalis>; 2015.
26. Sheldrick, G. M. *Acta Crystallogr. A*, **2008**, *64*, 112-122. DOI: 10.1107/S0108767307043930
27. Sheldrick, G. M. *Acta Crystallogr. C – Struct. Chem.*, **2015**, *71*, 3-8. DOI: 10.1107/S2053229614024218
28. Dolomanov, O. V.; Bourhis, L. J.; Gildea, R.J.; Howard, J. A. K.; Puschmann, H. *J. Appl. Crystallogr.*, **2009**, *42*, 339-341. DOI: 10.1107/S0021889808042726
29. Kohn, W.; Sham, L. J. *Phys. Rev.*, **1965**, *140*, A1133. DOI: 10.1103/PhysRev.140.A1133.
30. Frisch, M. J.; Trucks, G. W.; Schlegel, H. B.; Scuseria, G. E.; Robb, M. A.; Cheeseman, J. R.; Scalmani, G.; Barone, V.; Petersson, G. A.; Nakatsuji, H.; Li, X.; Caricato, M.; Marenich, A. V.; Bloino, J.; Janesko, B. G.; Gomperts, R.; Mennucci, B.; Hratchian, H. P.; Ortiz, J. V.; Izmaylov, A. F.; Sonnenberg, J. L.; Williams-Young, D.; Ding, F.; Lipparini, F.; Egidi, F.; Goings, J.; Peng, B.; Petrone, A.; Henderson, T.; Ranasinghe, D.; Zakrzewski, V. G.; Gao, J.; Rega, N.; Zheng, G.; Liang, W.; Hada, M.; Ehara, M.; Toyota, K.; Fukuda, R.; Hasegawa, J.; Ishida, M.; Nakajima, T.; Honda, Y.; Kitao, O.; Nakai, H.; Vreven, T.; Throssell, K.; Montgomery Jr., J. A.; Peralta, J. E.; Ogliaro, F.; Bearpark, M. J.; Heyd, J. J.; Brothers, E. N.; Kudin, K. N.; Staroverov, V. N.; Keith, T. A.; Kobayashi, R.; Normand, J.; Raghavachari, K.; Rendell, A. P.; Burant, J. C.; Iyengar, S. S.; Tomasi, J.; Cossi, M.; Millam, J. M.; Klene, M.; Adamo, C.; Cammi,

R.; Ochterski, J. W.; Martin, R. L.; Morokuma, K.; Farkas, O.; Foresman, J. B.; Fox, D.
J. Gaussian 16. Revision A. 03. Wallingford: Gaussian, 2016.

31. Becke, A.D. *J. Chem. Phys.*, **1993**, *98*, 5648-5652. DOI: 10.1063/1.464913.

32. Chemcraft, version 1.7, **2013**: <http://www.chemcraftprog.com>